Finite Element Simulation and Analysis of RC Beams with Modified Stirrups

Bonjoebee Bello[1*], *Orlean* Dela Cruz[2]

[1]Tarlac State University, Romulo Blvd., San Vicente, Tarlac City, 2300, Tarlac, Philippines
[2]Graduate School, Polytechnic University of the Philippines, Sta. Mesa, 1016, Metro Manila, Philippines

Abstract. This paper uses the finite element simulation to examine the effects of modified stirrups on RC beams. There are seventeen (17) FE models, including various stirrup configurations such as traditional, spiral, and truss systems, as well as advanced modifications, were thoroughly analyzed using Abaqus software to evaluate parameters such as load-deflection relationship, ductility, strength, failure modes, and crack patterns. Among these models, the BT-X design with a 125 mm spacing inclination of 72.10° demonstrated a remarkable load capacity of 110.856 kN, outperforming BN by 7.637%. Notably, throughout the simulation, the BT-R and BT-X designs were shown to be effective at increasing load-carrying capacity. Stirrup spacing and inclination angles are essential influences on RC beam performance. Specifically, the BT-X 125 design significantly improved flexural capacity and ductility. Furthermore, a uniform failure mode was identified across all models, highlighting the positive effect of modified stirrups on RC beam behavior. These findings highlight the importance of changing the stirrup design and selecting spacing and inclinations to improve RC beam performance.

1 Introduction

Regular reinforced concrete (RC) beams typically utilize longitudinal bars to prevent concrete from bending and stirrups to hold the longitudinal bars in place. They are commonly used for shear reinforcement alone [1]. However, the standard vertical stirrups, often in the form of two-legged configurations, are prone to unwinding under beam loading conditions, thus compromising the beam's strength [2]. Moreover, the traditional closed stirrups necessitate two end hooks for proper anchorage, resulting in additional steel weight and unnecessary construction costs and time[3]. Furthermore, research indicates that vertical stirrups might limit shear capacity due to the high compression stresses induced in the concrete stress field [4].

Shear failure is the most destructive and complicated failure mode of RC beams [5]. It is undesirable for engineers due to its abrupt occurrence with a brittle failure approach [6]. As a result, a significant urge has been made to improve RC beams' strength, which is led by the demand for structural safety [7].

* Corresponding author: brbello@tsu.edu.ph

Several researchers developed numerous strategies for enhancing and assessing several significant aspects of the behavior of RC beams [4]. However, most of these methods are centered on additives [8–12], partial or complete replacement of basic concrete materials [6], [13–21], recycling materials [22–24], or research on the size impact of RC beams [5]. On the other hand, modifying the configurations of the typical shear reinforcement of RC beams in terms of inclination and geometry is a new challenge and promising technique for improving RC beam strength [14–20].

According to the reviewed literature [7], changing conventional shear reinforcement to spiral and truss systems improves the shear and flexural strengths of RC beams. However, the present designs mostly use continuous rectangular spiral and truss systems, emphasizing the significance of exploring various configurations, inclinations, and spacings to establish the most effective design. Although the present designs of modified stirrups have demonstrated sound conclusions separately, there needs to be more comparison between the two, highlighting the importance of analyzing various modification designs to predict probable challenges for each design.

This study utilized ABAQUS software to simulate 17 Finite Element (FE) models of RC beams with the normal stirrup, present modified stirrups as shown in Fig. 1, and advanced stirrup modifications. This study aims to assess the impact of changes in the stirrups on the strength of RC beams by analyzing the relationship between load and midspan deflection, determining the ductility, and identifying failure mode and crack patterns. The current study's Finite Element Analysis (FEA) results were validated by simulating a model based on literature [32], using the same approach as simulating the FE models in this study – and then comparing the results to those obtained from the same literature source. The present study aims to significantly contribute to the existing literature by understanding the critical effects of modified stirrups on the strength and behavior of RC beams.

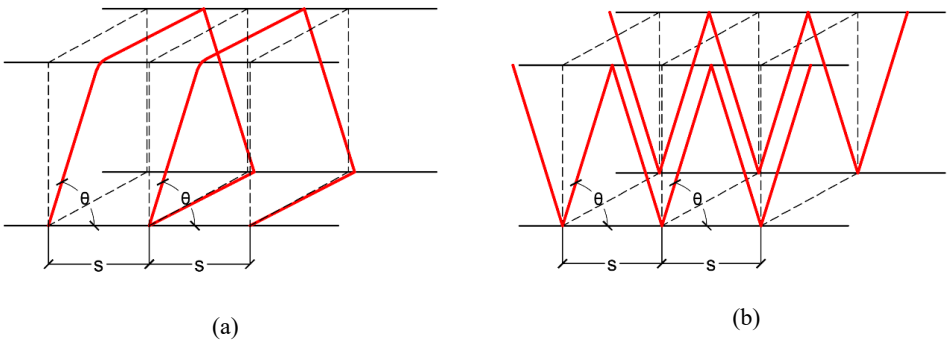

Fig. 1. Present Design of Modified Stirrups: (a) Spiral and (b) Truss System. [7]

2 Finite Element Method

Finite Element Method (FEM) is a numerical analysis methodology that provides approximate solutions to various engineering problems. It gives a nonlinear analysis of the system of equations to the FE model problems. The core premise of FEM is a solution zone that can be analytically described by replacing it with a set of discrete elements known as discretization. Furthermore, these components can be combined to create highly complicated geometrical shapes or forms [33]. These features of FEM help any researcher to design complex FE models.

Furthermore, FEM is one of the most precise and practical approaches to analyzing complicated structural engineering problems, which gives a convenient and flexible tool for

solving the issues related to the RC members' analyses [34]. The FEM has made significant promises in several mechanical applications associated with civil engineering structural modeling [35]. Six leading companies offer commercial software for finite element analyses, such as ABAQUS, ANSYS, SDRC-Ideas, RASNA, and MSC/NASTRAN [33]. ABAQUS [36, 37] and ANSYS [15, 38] are used by various researchers to model and study the effect of spiral and truss reinforcement on RC beams.

The experimental approach to evaluating the mechanical behavior of RC beams is considered helpful in developing results [36]. However, this approach has disadvantages regarding time and budget, as laboratory testing is costly and not immediately accessible [35] to researchers and requires more labor. The numerical method, in contrast, expends less cost and time and can also assist in obtaining an excellent understating of the behavior of RC beams [36].

The literature evaluating the RC beam behavior using modified stirrups is based on studies that have almost been performed through experimental research. Researchers making experimental approaches tend to need help preparing the specimens, performing laboratory tests, managing the time and budget of the study, and having more labor work compared with FE analysis, an alternative investigation method for the performance of RC beams [39]. Furthermore, using numerical approaches allows for improved comprehension of the behavior of RC beams while saving time and money compared to doing experimental research [36]. Moreover, the comparison of experimental and numerical data with the analytical calculation studied in 2016 demonstrates that the proposed FEM-based model may provide a reliable and reasonably accurate assessment of the behavior of RC beams [40].

3 Methodology

After a comprehensive review of the literature related to the study, the researcher identified significant variables influencing the modification of shear reinforcement in RC beams. These modifications are primarily concerned with alterations in geometry and inclinations. Within the scope of this study, two separate modified designs were identified: spiral and truss systems. Furthermore, the researcher expanded the study's scope by including advanced stirrups with an X-shaped geometry.

The present study simulated 17 FE models, including the Normal beam as the control variable with standard vertical stirrups (BN), identified the design of modified stirrups such as Spiral stirrups (BR-S) and rectangular Truss system (BT-R) and advanced stirrups such as vertical X-shaped stirrups (BV-X) and X-shaped truss system (BT-X). The FE models will be analyzed through a Four-Point Bending setup using Abaqus software to obtain the load capacity, midspan deflection, ductility, failure mode, and crack patterns. The results in the present study were verified by simulating a model based on literature, using the same approach as simulating the FE models in this study – and then comparing the results to those obtained from the same literature source. After validation, all findings will be statistically analyzed to establish the significance of beams with modified shear reinforcement against the normal beam. The study will then conclude and recommend improvement parameters based on the assessment of the results. Fig. 2 depicts the study's conceptual framework.

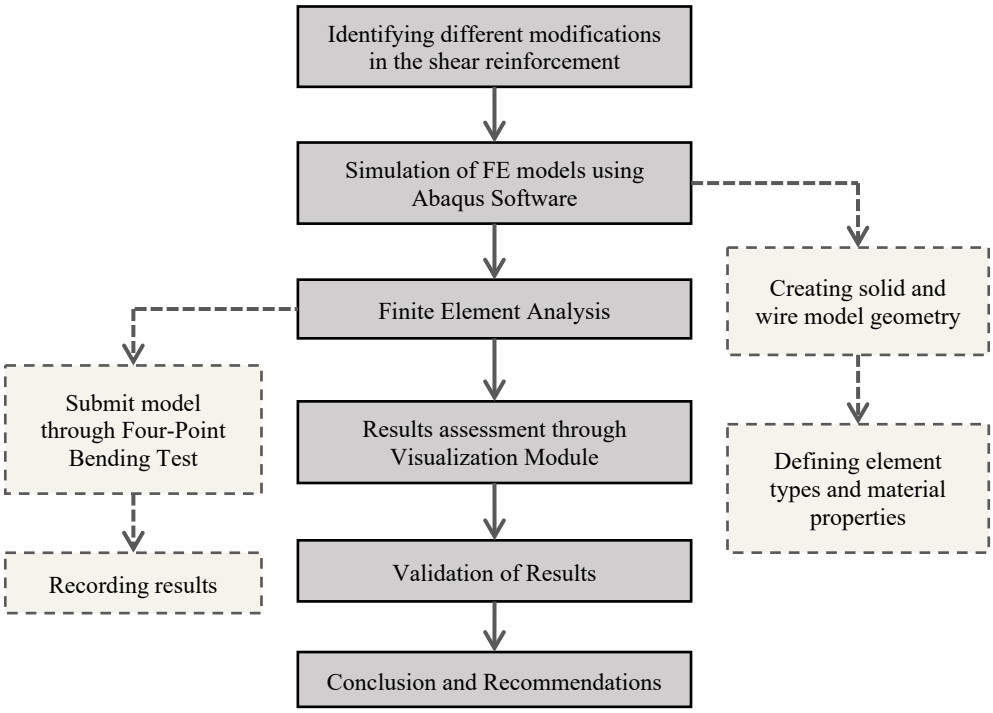

Fig. 2. The Conceptual Framework for the Simulation and Analysis of RC Beams with Modified Transverse Reinforcement.

3.1 Finite Element Models

3.1.1 Parts

The present study used a rectangular beam with the dimension of 200 x 300 x 2500 mm. 17 FE models have been simulated including the normal beam (BN) as the control model with the traditional shear reinforcement as shown in Fig. 3(a) and four modifications: individual X shaped vertical stirrups (BV-X) as shown in Fig. 3(b), continuous rectangular spiral (BR-S) as shown in Fig. 3(c), rectangular truss reinforcement system (BT-R) in Fig. 3(d), and X-shaped truss system (BT-X) in Fig. 3(e). Longitudinal bars were 16 mm in diameter, while various stirrups used 10 mm in diameter. Stirrup spacing ranged from 150 mm to 75 mm, and inclinations ranging from 68.53° to 80.13° were applied to specific modifications, referencing the x-axis due to the control beam's vertical stirrups.

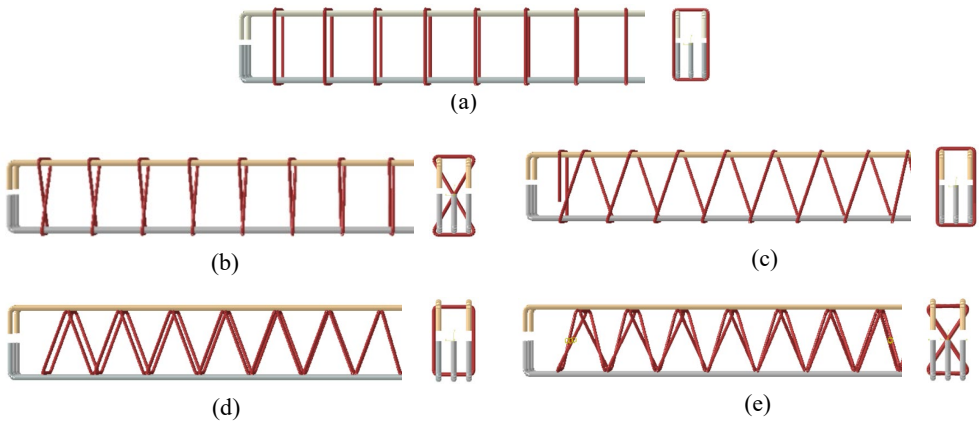

Fig. 3. Shear Reinforcement for Various Models.

3.1.2 Property

The researcher created three materials: concrete damage, steel bar, and steel support, using the Material Manager. The present study adopted the Concrete Damage Plasticity (CDP) model to establish the elastic and plastic material response, flow role, and yield surface evolution. The study used 29.10 MPa for the compressive strength of concrete, 235 MPa yield strength, and an ultimate strength of 410 MPa for all steel bars tabulated in Table 1.

Table 1. Material Properties.

Concrete		**Steel Reinforcement**	
Compressive Strength	29.10 MPa	Yield Strength	235 MPa
Young Modulus	20,111 MPa	Young Modulus	200,000 MPa
Poisson Ratio	0.20	Poisson Ratio	0.30
Density	2,000 kg/m^3	Density	7,850 kg/m^3

3.1.3 Assembly

The researcher assembled the RC beam, impactor, and support parts into a Four-Point Bending Test Setup. Precisely, the support part was positioned 150 mm from the edge of the beam part, and the impactors were placed 850 mm from the support and 500 mm apart from each other. The researcher used a Global Size of 50 mm and a finer mesh size of 25 mm to capture crack patterns of the beam part, as shown in Fig. 4. The reinforcement bars were set to a size of 20 mm, and the impactor retained the default size. For the element type, the researcher used Explicit, Linear, and 3D stresses for all solid elements, and for the reinforcement bars, Explicit, Linear and Truss Elements were used.

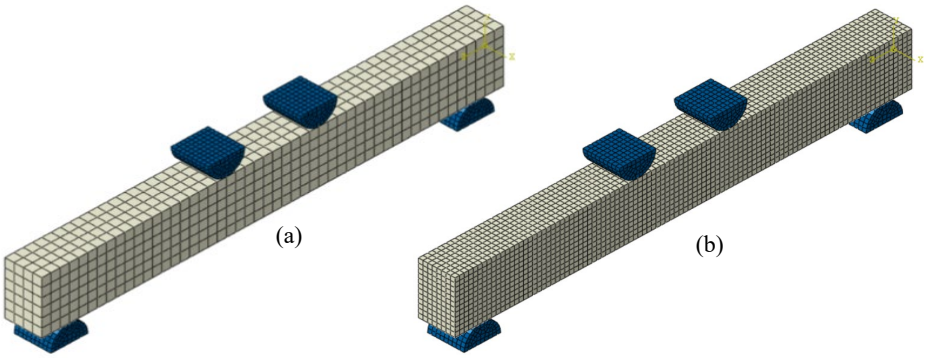

Fig. 4. The Assembly with (a) a 50 mm Mesh size and (b) a 25 mm Mesh Size for the Beam.

3.2 Finite Element Analysis

The FE models were loaded under a four-point bending test through Abaqus software with a 2200 mm space hinge-roller support to allow horizontal translation and rotation. As illustrated in Fig. 5, two loading points are placed in the midspan of the beam, 500 mm apart. This testing determined the force necessary to bend a beam under a four-point loading system, midspan deflection, and failure mode.

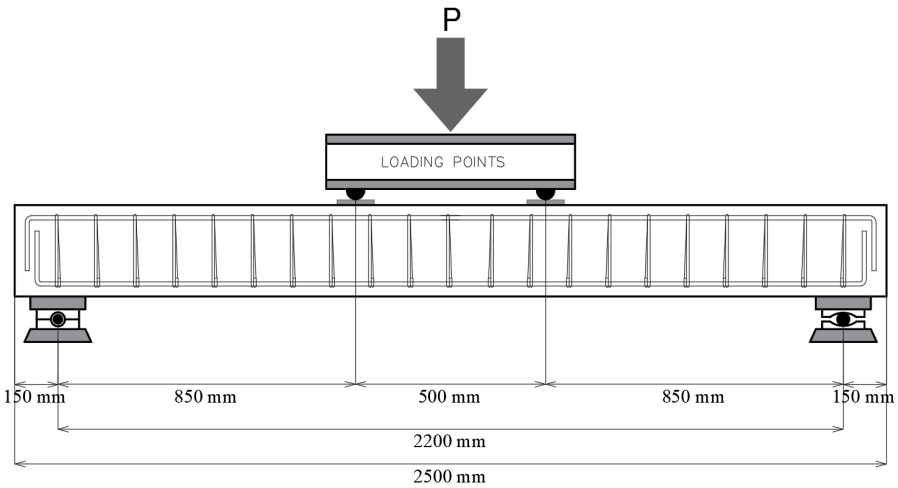

Fig. 5. Test Setup of RC Beams in Four-Point Bending Test.

3.2.1 Interaction

The researcher established the Interaction Property using the General Contact (Explicit) type and Dynamic Explicit approach. Tangential Behavior with a Friction Coefficient of 0.35 was implemented for the Contact Property. These configurations were essential for ensuring precise contact interactions and replicating the intended behavior of the model components during the analysis. Additionally, a Coupling Constraint was created in the Impactor to couple various degrees of freedom. This constraint facilitated the imposition of displacements in the Load Module, ensuring synchronized behavior throughout the analysis.

Furthermore, reinforcement bars were configured as Embedded elements within the beam model, integrating them into the structure rather than treating them as separate entities. This strategy aimed to capture the reciprocal influence and interaction between the beam and the embedded reinforcement, enhancing the accuracy of their combined behavior during the analysis. The interaction properties are illustrated in Fig. 6.

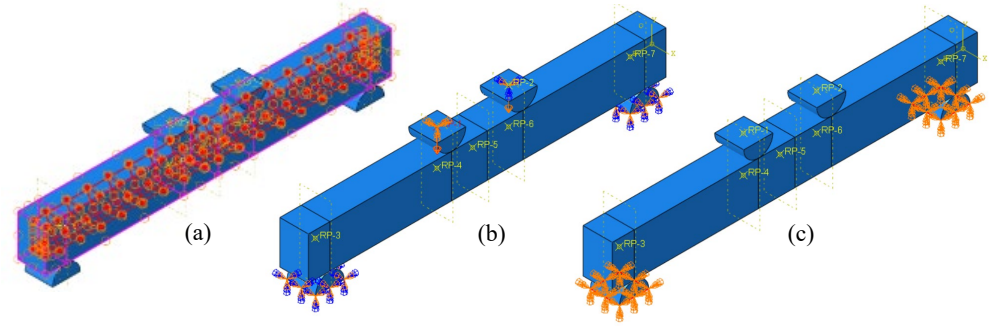

Fig. 6. (a) Constraint Property of the Rebar Embedded in Beam, (b) Boundary Condition (Displacement) Applied in the Impactors, and (c) Boundary Condition (Fixed) Applied in the Supports.

3.2.2 Step

In this module, the researcher used a period of 2 with a Frequency of 0.02 to obtain 100 offsets in the results. Integrated Output Sections are created to obtain the midspan deflection and the corresponding load in each deflection.

3.2.3 Load

The Displacement Method was used in this study to calculate the maximum deflection and the accompanying load. Figures 6 (a) and (b) depict the Displacement/Rotation Type Boundary Condition, which was applied to the impactors and is equivalent to -40 mm of U2 (Global y-axis). All other borders, such as U1 (Global x-axis), U3 (Global z-axis), UR1 (Y-axis Rotation), UR2 (X-axis Rotation), and UR3 (Z-axis Rotation), are set to 0. The researcher implemented a fixed boundary condition for the supports. This means that the displacement (movement) in all directions (U1 to UR3) at these locations was constrained and fixed at 0. By applying this condition, the Supports were immobilized and prevented from moving in any direction, ensuring they remained stable and stationary throughout the simulation or analysis. This fixed boundary condition is commonly used in structural and mechanical analyses to represent rigid supports or fixed connections, providing a realistic representation of actual scenarios.

3.2.4 Job

The researcher designated the Job as "4-point-bending-test- (Name of the model)" with a Full Analysis Job Type. The researcher employed parallelization to advance the analysis process, utilizing multiple processors. Furthermore, in Abaqus/Explicit Precision, the Double - Analysis + Packager approach was used to optimize the analysis duration, ensuring the process was completed efficiently without unnecessary delays.

4 Results and Discussions

The objective of the present study was to obtain the load-carrying capacity, midspan deflection, ductility, strength, failure mode, and crack patterns of the beams.

4.1 Load Capacity and Midspan Deflection Relationship

This study investigated the load capacity and midspan deflection across five distinct groups: BN, BV-X, BR-S, BT-R, and BT-X. The findings revealed that the control beam, BN, initiated yielding at a load of 96.308 kN, accompanied by a displacement of 12.00 mm. As the load continued to increase, there was a gradual rise in displacement with only a slight increment in the applied load on the beam. Ultimately, at a displacement of 22.00 mm, the BN beam reached its failure load of 102.991 kN.

Regarding overall performance among the independent variables, the BT-X group had the highest load capacity, particularly at a spacing of 125 mm. Specifically, the BT-X 125 beam began its yielding phase at 100.958 kN at a displacement of 14.00 mm. Afterward, the load steadily grew as displacement ascended. Notably, the load peaked at 103.961 kN when the displacement reached 24.00 mm before ultimately failing at 110.856 kN at 30.00 mm displacement.

Fig. 7.0 displays the correlation between BV-X Group models and the control model, BN, which has a load capacity of 102.991 kN and a midspan deflection of 22 mm. BV-X 150 and BV-X 125 have slightly higher load capacities than BN, with load capacities of 104.970 kN and 104.302 kN, respectively. Additionally, BV-X 150 can also handle a significant displacement with a value of 26.00 mm while carrying its respective capacity higher than BN.

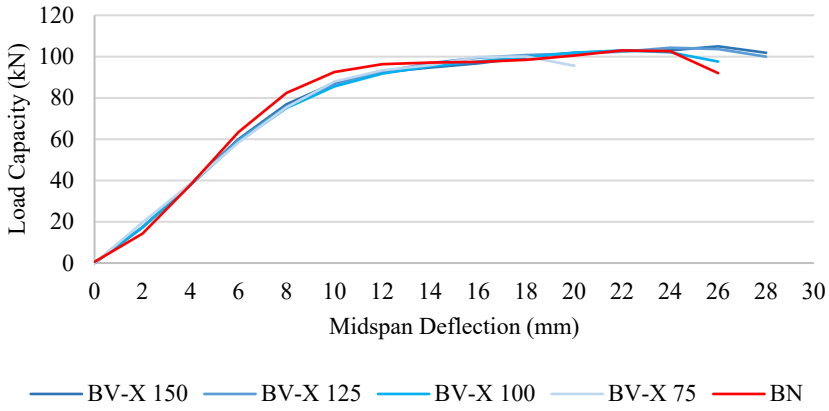

Fig. 7. Load Capacity vs Midspan Deflection Graph between BV-X Group and BN.

Fig. 8.0 displays the correlation between the BR-S Group models and the control model, BN. The study reveals that decreasing the spacing between spiral stirrups enhances load capacity across all BR-S variants. The BR-S 75 type exhibits the highest load capacity at 105.824 kN, with a more significant deflection of 30.00 mm compared to BN's 22.00 mm. These findings highlight the effectiveness of reducing stirrup spacing in BR-S models to improve load capacity while carrying a more significant deflection.

Fig. 9.0 compares the BT-R Group models and the control model, BN. Among the BT-R groups with different stirrup spacings (150, 125, 100, and 75 mm), BT-R 125 and 100 had the highest load capacities, exceeding BN with the magnitude of 109.793 kN and 109.673 kN, respectively. Furthermore, BT-R 125 and 150 outperformed the group, withstanding a

displacement of 30.00 mm. In summary, the rectangular truss stirrups outperformed the conventional beam in load capacity, with BT-R 125 and BT-R 100 performing exceptionally well.

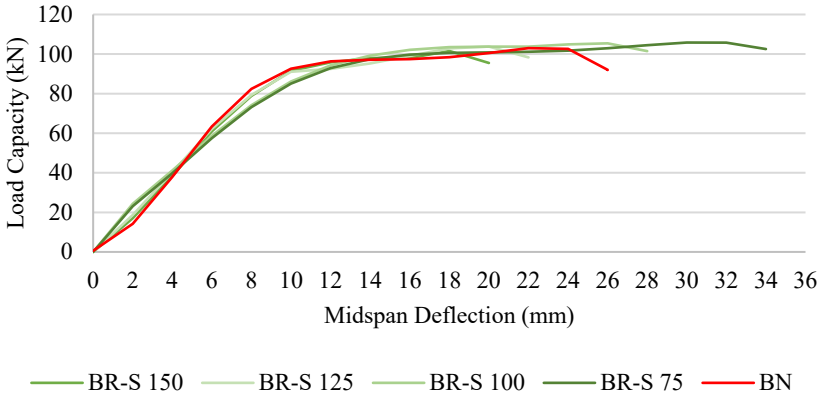

Fig. 8. Load Capacity vs Midspan Deflection Graph between BR-S Group and BN.

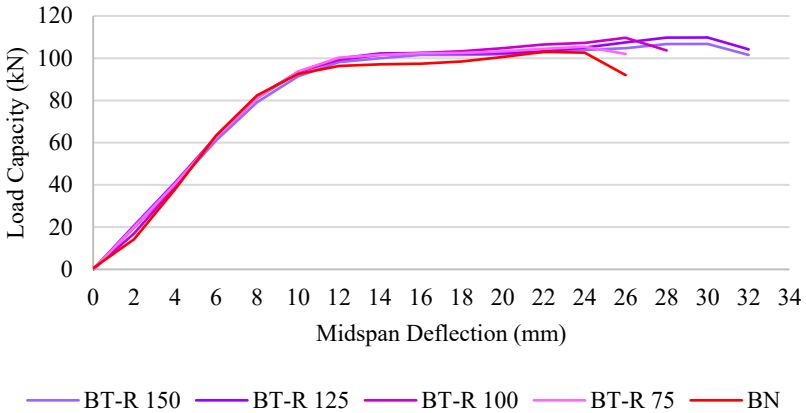

Fig. 9. Load Capacity vs Midspan Deflection Graph between BT-R Group and BN.

Fig. 10.0 illustrates the relationship between the BT-X group models and the control, BN. The BT-X groups achieved various outcomes with stirrup spacings of 150, 125, 100, and 75 mm. The BT-X 125 beam had the highest load capacity at 110.856 kN. Furthermore, the BT-X 125 beam demonstrated more robust durability, withstanding a more significant deflection of 30.00 mm than BN, demonstrating its potential for improved structural integrity under loading circumstances.

Fig. 11.0 demonstrates an evident contrast between the BV-X and BR-S groups regarding spacing characteristics. Specifically, the BV-X group shows a decrease in load capacity with lessening spacing, whereas the BR-S group shows an increase in load capacity under the same conditions. Furthermore, the BT-R group has better load capabilities in the 100 mm to 125 mm spacing range, while the BT-X group has higher load capacities in the 100 mm to 150 mm spacing.

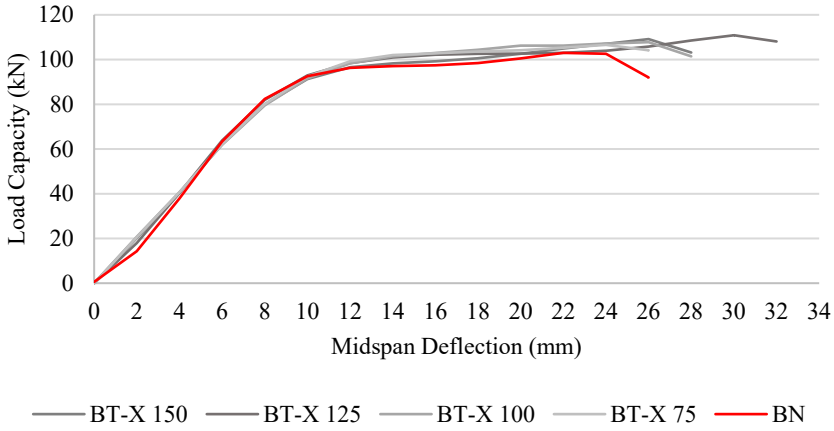

Fig. 10. Load Capacity vs Midspan Deflection Graph between BT-X Group and BN.

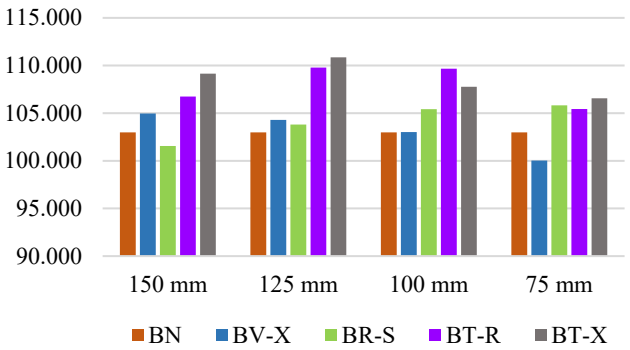

Fig. 11. Load Capacity for Each Group from Four Spacings.

The findings indicate that the behavior of the modified stirrups changes significantly depending on the spacing arrangement when loaded. Each spacing interval has a distinct effect on stirrup performance, influencing characteristics such as load-bearing capacity. It also emphasizes the significance of carefully assessing and selecting the optimal spacing arrangement for the application's requirements and limits.

4.2 Flexural Capacity

The current study narrowed down each model's failure mechanism to determine its strength. A thorough examination showed that the failure process in all models includes flexural stresses, indicating that the identified strength characteristics represent flexural strength rather than shear strength.

However, the researcher extended the scope of the present study by including advanced stirrups in X-shape geometry. The results showed that an X-shaped Truss reinforcement system with a 125 mm spacing and inclination of 72.10° is the optimal design for significantly improving RC beam flexural capacity. BT-X 125 has a flexural capacity of 110.856 kN, as listed in Table 2, and when compared to BN, it reveals a significant increase of 7.637%. This truss reinforcement system improved the flexural capacity of the RC beam since there was an additional flexural effect coming from the inclined stirrups. The truss stirrups reinforce

the longitudinal bars as the substitute concrete field [1]. This indicates that the truss reinforcement system provided an additional stiffness in the total stiffness of the concrete beams [1, 32]. Furthermore, the distribution of stresses in the X-shaped stirrup may incorporate axial and shear stresses, unlike the vertical stirrup, which primarily experiences axial stress.

Table 2. Summary of Load Capacity and Midspan Displacement at Yielding and Ultimate Stage.

Model	Yielding		Ultimate		Ductility Ratio (Δu/Δy)
	Load (Py)	Disp. (Δy)	Load (Pu)	Disp. (Δu)	
BN	96.3079	12.00	102.991	21.999	1.83
BV-X Group					
BV-X 150	92.3858	12.00	104.970	26.00	2.17
BV-X 125	99.4572	16.00	104.302	24.00	1.50
BV-X 100	97.6828	16.00	103.013	22.00	1.37
BV-X 75	95.9125	14.00	100.030	18.00	1.29
BR-S Group					
BR-S 150	95.806	12.00	101.556	18.00	1.50
BR-S 125	91.0838	10.00	103.808	20.00	2.00
BR-S 100	99.262	14.00	105.424	26.00	1.86
BR-S 75	99.7024	16.00	105.824	30.00	1.87
BT-R Group					
BT-R 150	98.1473	12.00	106.752	30.00	2.50
BT-R 125	99.9225	12.00	109.793	30.00	2.50
BT-R 100	99.1914	12.00	109.673	26.00	2.17
BT-R 75	100.267	12.00	105.443	24.00	2.00
BT-X Group					
BT-X 150	96.548	12.00	109.143	26.00	2.17
BT-X 125	98.4516	12.00	110.856	30.00	2.50
BT-X 100	98.2898	12.00	107.773	26.00	2.17
BT-X 75	99.2063	12.00	106.564	24.00	2.00

4.3 Ductility

The ductility of a beam, defined as its ability to withstand elastic deformation without reducing its load-bearing capacity until failure [41], is critical in RC structures. This essential parameter, calculated by dividing the peak-to-yield displacement [42], indicates structural integrity. Ductility, defined as deformation or energy considerations, takes several forms, including deflection, strain, and curvature [43].

In this study, the ductility ratio was determined by calculating the displacement ratio at yield to that at the ultimate stage. Table 1 illustrates that the control beam BN exhibits a ductility ratio exceeding 1.0, precisely 1.83, signifying ductile behavior. Conversely, within the BV-X group, all models also display ductility ratios surpassing 1.0, indicating ductile

behavior. However, only one under BV-X increased in ductility, specifically the BV-X 150, suggesting that these designs within the BV-X group are comparatively more ductile than BN. It is evident that when the spacing gets smaller, the beam's ductility under BV-X decreases. Moving to the BR-S group, only the BR-S 150 design is less ductile than BN, while the BR-S 125 beam shows the highest level of ductility within this group.

Moreover, BT-R and BT-X groups showcased more ductile behavior within the truss reinforcement system, surpassing BN's ductility. This suggests that all models within these two groups outperformed BN and exhibited prolonged endurance before failure. Specifically, BT-R 150, BT-R 125, and BT-X 125 are the most ductile designs from the two groups.

Fig. 12 shows that the BV-X group's ductility ratio drops as the spacing narrows. In contrast, the BR-S group exhibits maximum ductility levels from 75 mm to 125 mm spacing. Furthermore, the BT-R group has higher ductility than the BN group, which is particularly noticeable at spacings of 150 mm. Finally, the models in the BT-X group exhibit more ductility than BN, which is especially noticeable at 125 mm spacing.

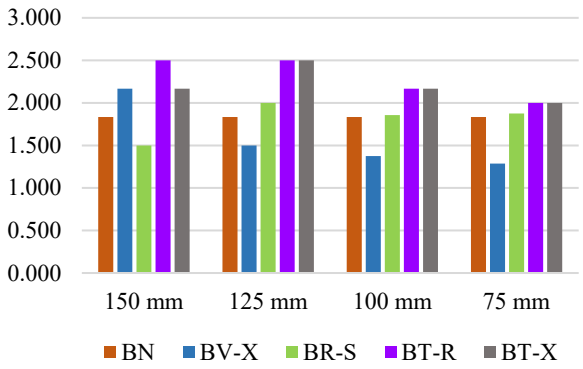

Fig. 12. Ductility of Each Model from Four Spacings.

4.4 Failure Mode and Crack Patterns

In the study of Joshy and M (2017) [44] and Shatarat et al. (2018) [3], the crack patterns and the failure mechanism for the standard beam and that of modified stirrups were almost the same. Similarly, in the present study, a consistent failure mode characterized by uniform flexural tension was observed in all analyzed models. It tested specimens in the present study, as illustrated in Fig. 13 to Fig. 17. The failure began with the yielding of the steel reinforcement, followed by the subsequent crushing of concrete at the compression fiber of the beam. The development of cracks along the tension fiber was evident, progressively extending towards the compression side with the increasing applied load and slowly inclined towards the neutral axis of the beams.

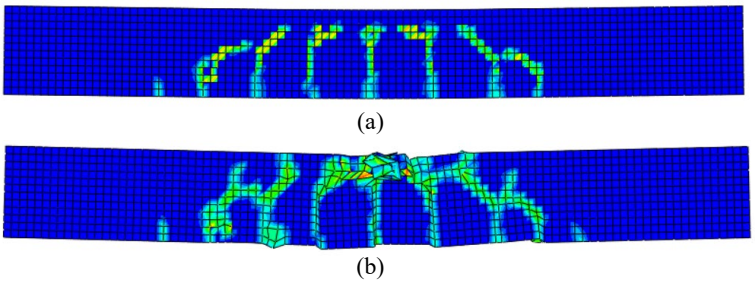

Fig. 13. Crack Patterns in BN for a) Flexural Cracks before Failure and b) Failure Mode of BN when concrete crushed at compression side.

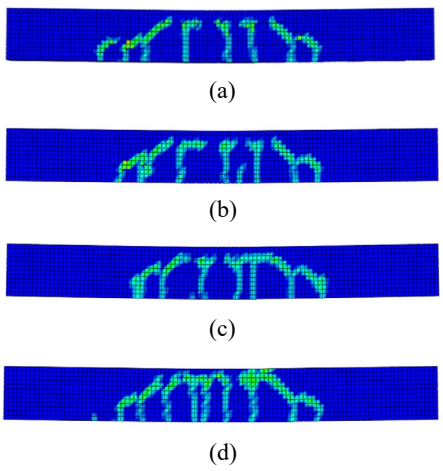

Fig. 14. Crack Patterns of BV-X Group from 150 mm to 75 mm spacing.

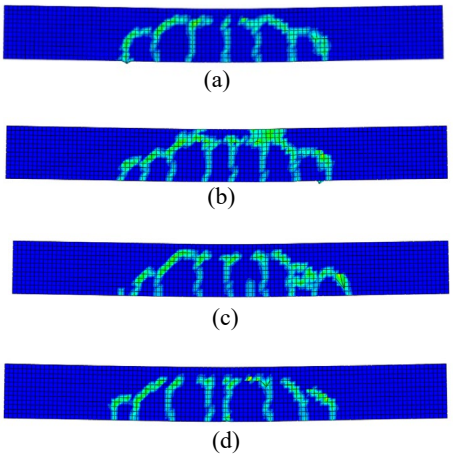

Fig. 15. Crack Patterns of BR-S Group from 150 mm to 75 mm spacing.

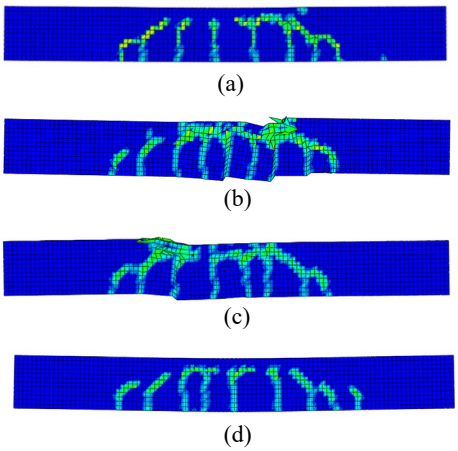

Fig. 16. Crack Patterns of BT-R Group from 150 mm to 75 mm spacing.

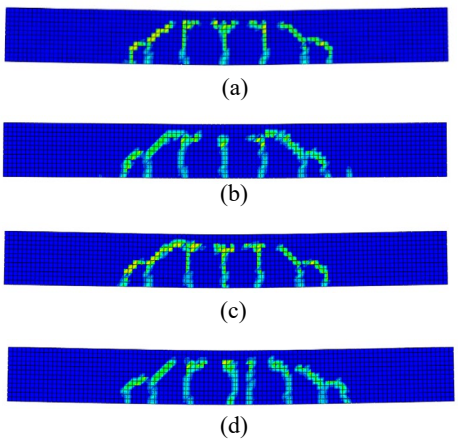

Fig. 17. Crack Patterns of BT-X Group from 150 mm to 75 mm spacing.

5 Results Assessment

5.1 Comparison of the Present study to the Literature

Because the present study did not include actual testing, a model was simulated based on the literature [32], and the findings were compared to those described in the literature. The model used was Beam BN, and the literature indicated a failure load of 28.11 kN; however, in the present study, it was found to be 27.22 kN. The predicted failure load of ABAQUS was 3.17% lower than the experimental value.

5.2 Statistical Analysis

The researcher used Jamovi [45, 46] software to run One-Way ANOVA to assess the significance of differences in the load capacities of the normal beam (as the dependent variable) with the independent variables (BV-X, BR-S, BT-R, and BT-X).

As shown in Table 3, the resulting p-value is less than 0.001, indicating a significant difference in load capacity between beams with modified stirrups and the normal beam. This statistical finding emphasizes the effect of stirrup modifications on the beams' structural integrity and load-bearing capacity.

In the Tukey post-hoc test in Table 4, more asterisks imply more significant differences between variables. It shows that when BN is compared to the four groups, the BT-X groups have a noticeable asterisk with a more excellent mean difference value. This indicates that the load capacity of BN is significantly different from that of the BT-X groups, implying a considerable increase in structural performance between these categories. The enormous mean difference and the appearance of more asterisks demonstrate the BT-X modification's significant influence on enhancing the beams' load-bearing capacities compared to other groups.

Table 3. One-Way ANOVA Results.

One-way ANOVA (Fisher's)				
	F	df1	df2	p
LOAD CAPACITY	8.77	4	15	<0.001

Group Descriptives					
	BEAM MODEL	N	Mean	SD	SE
LOAD CAPACITY	BN	4	103	0.00	0.000
	BV-X	4	103	2.19	1.094
	BR-S	4	104	1.94	0.968
	BT-R	4	108	2.17	1.083
	BT-X	4	109	1.85	0.923

Table 4. Post Hoc test results.

Tukey Post-Hoc Test - LOAD CAPACITY						
		BN	BV-X	BR-S	BT-R	BT-X
BN	Mean difference	-	-0.0877	-1.160	-4.92*	-5.593**
	p-value	-	1.000	0.892	0.012	0.005
BV-X	Mean difference		-	-1.07	-4.84*	-5.505**
	p-value		-	0.916	0.014	0.005
BR-S	Mean difference			-	-3.76	-4.431*
	p-value			-	0.069	0.026
BT-R	Mean difference				-	-0.669
	p-value				-	0.984
BT-X	Mean difference					-
	p-value					-

*Note. *p <.05, **p<.01, ***p<.001*

6 Conclusions and Recommendations

This study involved simulating 17 FE Models of RC beams using ABAQUS to assess the impact of modified stirrups on beam strength. This study includes the normal beam (BN), beams with Spiral stirrups (BR-S) and rectangular Truss system (BT-R), and beams with advanced stirrups such as vertical X-shaped stirrups (BV-X) and X-shaped truss system (BT-X). It aimed to determine the load-midspan deflection relationship, ductility, strength, failure modes, and crack patterns. The researcher validated simulation findings by simulating a model from the literature and comparing its results with the literature findings. Subsequent conclusions are taken from the simulation and discussions:

1. With 125 mm spacing, the BT-X design is the most effective, with a flexural capacity of 110.856 kN, 7.637% higher than the standard beam. A comprehensive study of this type of modification, considering varied load scenarios, is recommended to learn how these configurations respond to different levels and types of loading.
2. Vertical X-shaped stirrups, Spiral, and rectangular and X-shaped truss stirrups all enhance load-carrying capacity compared to BN. However, BT-R and BT-X consistently outperform others, significantly improving load capacity and deflection. In-depth analysis should delve into the underlying mechanisms of these configurations, examining their potential application across various structural scenarios and contexts.
3. Stirrup spacing significantly influences RC beam load-carrying capacity per modification design. BV-X performs best at wider spacing but weakens at smaller spacing. BR-S, on the other hand, performed well with stiffer spacing. Meanwhile, BT-R and BT-X excel at both in 125 mm spacing. Also, the optimal inclination angle is 72.10°, enhancing load capacity and durability. These findings highlight the relevance of stirrup spacing in determining the type of modification to improve RC beams' efficiency.

4. Most designs tend to enhance ductility compared to BN. In the BV-X group, reduced stirrup spacing was shown to reduce ductility, but in the BR-S group, stiff spiral spacing led to increased ductility. Among these groups, the BT-R 150, BT-R 125, and BT-X 125 designs were the most ductile, with a 36.612% increase higher than BN. These findings suggest that ductility performance varies depending on modification type and stirrup spacing.
5. All analyzed models, including BN, had a uniform failure mode defined by flexural tension failure. This demonstrates the effectiveness of the modified stirrups on RC beam behavior. Nonetheless, the current study suggests applying a finer mesh size to examine more of the crack propagation throughout the simulation.
6. The slight difference between the predicted failure load by ABAQUS and the observed experimental result indicates areas for refining the simulation in the present study. Investigating these factors can enhance simulation accuracy and deepen our understanding of structural mechanics behavior under load, facilitating ongoing improvement in this field.
7. While the FEA findings have been verified by comparing the simulation results of the beam BN in the literature, it is still recommended to conduct an actual experiment and compare the actual results from the simulation, which will aid in establishing the validity and reliability of the present study.

References

1. R. Djamaluddin, P. L. Frans, and R. Irmawati, "Flexural Capacity of the Concrete Beams Reinforced by Steel Truss System," MATEC Web of Conferences, vol. **138**, pp. 1–8, Dec. (2017), doi: 10.1051/MATECCONF/201713802003.
2. Karunanidhi.S, "INVESTIGATION ON SPIRAL STIRRUPS IN REINFORCED CONCRETE BEAMS," International Journal of Novel Research in Civil Structural and Earth Sciences, vol. **6**, no. 3, pp. 14–28, 2019, Accessed: Aug. 03, (2022). [Online]. Available: www.noveltyjournals.com
3. N. Shatarat, H. M. Mahmoud, and H. Katkhuda, "Shear capacity investigation of self compacting concrete beams with rectangular spiral reinforcement," Constr Build Mater, vol. **189**, pp. 640–648, Nov. (2018), https://doi.org/10.1016/j.conbuildmat.2018.09.046
4. P. Colajanni, L. La Mendola, G. Mancini, A. Recupero, and N. Spinella, "Shear capacity in concrete beams reinforced by stirrups with two different inclinations," Eng Struct, vol. **81**, no. 1, pp. 444–453, Dec. (2014), doi: 10.1016/j.engstruct.2014.10.011.
5. L. Jin, T. Wang, X. ang Jiang, and X. Du, "Size effect in shear failure of RC beams with stirrups: Simulation and formulation," Eng Struct, vol. **199**, p. 109573, Nov. (2019), https://doi.org/10.1016/j.engstruct.2019.109573
6. W. Mansour and B. A. Tayeh, "Shear Behaviour of RC Beams Strengthened by Various Ultrahigh Performance Fibre-Reinforced Concrete Systems," Advances in Civil Engineering, vol. **2020**, no. 3, pp. 1–18, Jul. (2020), https://doi.org/10.1155/2020/2139054
7. B. R. Bello and O. G. Dela Cruz, "Shear and Flexural Performance of Reinforced Concrete Beams with Modified Shear Reinforcement: A Literature Review," vol. **374**. (2024). https://doi.org/10.1007/978-981-99-4229-9_9
8. T. C. Herring, T. Nyomboi, and J. N. Thuo, "Ductility and cracking behavior of reinforced coconut shell concrete beams incorporated with coconut shell ash," Results in Engineering, vol. **14**, p. 100401, Jun. (2022), https://doi.org/10.1016/j.rineng.2022.100401

9. A. A. Ibrahim, N. H. AL-Shareef, M. H. Jaber, R. F. Hassan, H. H. Hussein, and N. H. Al-Salim, "Experimental investigation of flexural and shear behaviors of reinforced concrete beam containing fine plastic waste aggregates," Structures, vol. **43**, pp. 834–846, Sep. (2022), https://doi.org/10.1016/j.istruc.2022.07.019
10. S. A. Yıldızel et al., "Experimental investigation and analytical prediction of flexural behaviour of reinforced concrete beams with steel fibres extracted from waste tyres," Case Studies in Construction Materials, vol. **19**, p. e02227, Dec. (2023), https://doi.org/10.1016/j.cscm.2023.e02227
11. N. Mejía, A. Sarango, and A. Espinosa, "Flexural and shear strengthening of RC beams reinforced with externally bonded CFRP laminates postfire exposure by experimental and analytical investigations," Eng Struct, vol. **308**, p. 117995, Jun. (2024), https://doi.org/10.1016/j.engstruct.2024.117995
12. C. Daniel, R. O. Onchiri, and B. O. Omondi, "Structural behaviour of reinforced concrete beams containing recycled polyethylene terephthalate and sugarcane bagasse ash," Applications in Engineering Science, vol. **18**, p. 100178, Jun. (2024), https://doi.org/10.1016/j.apples.2024.100178
13. W. T. Segui, Steel Design, 6th ed. (Cengage Learning, 2017).
14. J. A. Apeh and O. G. Okoli, "Evaluation of Ductility Index of Concrete Beams Reinforced with Rebars Milled from Scrap Metals," Concrete Research Letters, vol. **7**, no. 2, pp. 56–68, May (2016).
15. M. B. M and N. Vedic, "Shear Capacity of RC Beams with Different Patterns of Spiral Reinforcements," International Journal of Engineering Research & Technology, vol. **6**, no. 6, Apr. (2018), doi: 10.17577/IJERTCONV6IS06017.
16. F. F. Manggapis, S. D. A. Kumar, J. R. P. G. Lucena, A. P. I. Carabbacan, and O. G. Dela Cruz, "Advancements in Concrete Incorporation: Harnessing the Potential of Crumb Rubber Tires as Sustainable Alternatives to Fine Aggregates," (2023), pp. 195–205. doi: 10.1007/978-3-031-42588-2_16.
17. F. Cayanan, O. G. Dela Cruz, J. M. Jacinto, A. I. Sawadjaan, and A. A. Hawari, "Engineering Cementitious Composite as Seismic Isolation: A Review of Its Application as Bendable Concrete," (2024), pp. 163–175. doi: 10.1007/978-981-99-4229-9_15.
18. A. P. I. Carabbacan and T. A. Amatosa, "Effects of Polypropylene Fibers from Single-Use Facemasks on the Microstructure of Normal Cementitious Composites," (2023), pp. 183–193. doi: 10.1007/978-3-031-42588-2_15.
19. A. Saraswat, A. Kumar Parashar, and R. Bahadur, "Effect of coconut shell ash substitute with cement on the mechanical properties of cement concrete," Mater Today Proc, Nov. (2023), https://doi.org/10.1016/j.matpr.2023.11.014
20. P. Das, S. Chakraborty, and S. V. Barai, "Flexural behaviour of fly ash incorporated ferrochrome slag aggregate reinforced concrete beam," Journal of Building Engineering, vol. **76**, p. 107317, Oct. (2023), https://doi.org/10.1016/j.jobe.2023.107317
21. N. Bheel et al., "Effect of wheat straw ash as cementitious material on the mechanical characteristics and embodied carbon of concrete reinforced with coir fiber," Heliyon, vol. **10**, no. 2, p. e24313, Jan. (2024), https://doi.org/10.1016/j.heliyon.2024.e24313
22. F. Yu, M. Wang, D. Yao, and Y. Liu, "Experimental research on flexural behavior of post-tensioned self-compacting concrete beams with recycled coarse aggregate," Constr Build Mater, vol. **377**, p. 131098, May (2023), https://doi.org/10.1016/j.conbuildmat.2023.131098
23. D. Gao, F. Luo, Y. Yan, J. Tang, and L. Yang, "Experimental investigation on the flexural performance and damage process of steel fiber reinforced recycled coarse

aggregate concrete," Structures, vol. **51**, pp. 1205–1218, May (2023), https://doi.org/10.1016/j.istruc.2023.03.122
24. M. Elsayed, S. R. Abd-Allah, M. Said, and A. A. El-Azim, "Structural performance of recycled coarse aggregate concrete beams containing waste glass powder and waste aluminum fibers," Case Studies in Construction Materials, vol. **18**, p. e01751, Jul. (2023), https://doi.org/10.1016/j.cscm.2022.e01751
25. Y. Li, M. Wu, W. Wang, and X. Xue, "Shear Behavior of RC Beams Strengthened by External Vertical Prestressing Rebar," Advances in Civil Engineering, vol. **2021**, pp. 1–12, Mar. (2021), https://doi.org/10.1155/2021/5483436
26. D.-Y. Yoo and J.-M. Yang, "Effects of stirrup, steel fiber, and beam size on shear behavior of high-strength concrete beams," Cem Concr Compos, vol. **87**, pp. 137–148, Mar. (2018), https://doi.org/10.1016/j.cemconcomp.2017.12.010
27. L. Biolzi and S. Cattaneo, "Response of steel fiber reinforced high strength concrete beams: Experiments and code predictions," Cem Concr Compos, vol. **77**, pp. 1–13, Mar. (2017), https://doi.org/10.1016/j.cemconcomp.2016.12.002
28. G. Chethan, J. Sanjith, A. Ranjith, and B. M. Kiran, "Shear Strength Capacity of Normal and High Strength Concrete Beams Bonded by CFRP Wraps," International Journal of Engineering and Advanced Technology (IJEAT), vol. **4**, no. 1, Oct. (2014).
29. Y. Fritih, T. Vidal, A. Turatsinze, and G. Pons, "Flexural and shear behavior of steel fiber reinforced SCC beams," KSCE Journal of Civil Engineering, vol. **17**, no. 6, pp. 1383–1393, Sep. (2013), doi: 10.1007/s12205-013-1115-1.
30. S. M. Abd-Alla, W. W. Ibrahim, M. M. Hashem, and A. S. Eisa, "Shear strength of normal, medium and high strength reinforced concrete beams," pp. 1–26, Oct. (2017).
31. S.-W. Kim, "Prediction of Shear Strength of Reinforced High-Strength Concrete Beams Using Compatibility-Aided Truss Model," Applied Sciences, vol. **11**, no. 22, p. 10585, Nov. (2021), https://doi.org/10.3390/app112210585
32. H. Hamkah, "IMPROVING FLEXURAL MOMENT CAPACITY OF CONCRETE BEAM BY CHANGING THE REINFORCEMENT CONFIGURATION," International Journal of GEOMATE, vol. **20**, no. 79, pp. 161–167, Mar. (2021), doi: 10.21660/2021.79.j2042.
33. V. Jagota, A. P. S. Sethi, and K. Kumar, "Finite Element Method: An Overview, " WALAILAK JOURNAL, vol. **10**, no. 1, pp. 1–8, Jan. (2013), doi: 10.2004/wjst.v10i1.499.
34. S. H. Yang, K. S. Woo, J. J. Kim, and J. S. Ahn, "Finite Element Analysis of RC Beams by the Discrete Model and CBIS Model Using LS-DYNA," Advances in Civil Engineering, vol. **2021**, Feb. (2021), https://doi.org/10.1155/2021/8857491
35. F. Z. Bhat, "Application of Finite Element Analysis," in Application of Finite Element Analysis, Jun. 2021. Accessed: Aug. 07, 2022. [Online]. Available: https://www.researchgate.net/publication/352017598_Application_of_Finite_Element_Analysis
36. M. Arafa, M. A. Alqedra, and R. Salim, "Performance of RC beams with embedded steel trusses using nonlinear FEM analysis," Advances in Civil Engineering, vol. **2018**, (2018), https://doi.org/10.1155/2018/9079818
37. S. S. Chiriki and G. Sri Harsha, "Finite element analysis of RC deep beams strengthened with I-section and truss reinforcement," Mater Today Proc, vol. **33**, pp. 156–161, Jan. (2020), doi: 10.1016/J.MATPR.2020.03.579.
38. D. Dinesh and A. P, "Numerical Study of Hybrid Steel Trussed Concrete Beam," International Research Journal of Engineering and Technology (IRJET) , vol. **4**, no. 5, May (2017).

39. A. Demir, G. Dok, and H. Öztürk, "3D Numerical Modeling of RC Deep Beam Behavior by Nonlinear Finite Element Analysis," DISASTER SCIENCE AND ENGINEERING, vol. **2**, no. 1, pp. 13–18, Apr. (2016).
40. G. Campione, P. Colajanni, and A. Monaco, "Analytical evaluation of steel–concrete composite trussed beam shear capacity," Materials and Structures/Materiaux et Constructions, vol. **49**, no. 8, pp. 3159–3176, Aug. (2016), https://doi.org/10.1617/s11527-015-0711-6
41. Z. You, X. Chen, and S. Dong, "Ductility and strength of hybrid fiber reinforced self-consolidating concrete beam with low reinforcement ratios," Systems Engineering Procedia, vol. **1**, pp. 28–34, (2011), doi: 10.1016/j.sepro.2011.08.006.
42. R. Salih, F. Zhou, N. Abbas, and A. Khan Mastoi, "Experimental Investigation of Reinforced Concrete Beam with Openings Strengthened Using FRP Sheets under Cyclic Load," Materials, vol. **13**, no. 14, p. 3127, Jul. (2020), doi: 10.3390/ma13143127.
43. E. Natarajan, "DUCTILITY RESPONSE OF HYBRID FIBRE REINFORCED CONCRETE BEAMS," Journal of Urban and Environmental Engineering, pp. 174–179, Jun. (2018), https://doi.org/10.4090/juee.2017.v11n2.174-179
44. V. Joshy and K. M. Faisal, "Experimental Study on the Behaviour of Spirally Reinforced SCC beams," International Journal of Engineering Research and General Science, vol. **5**, no. 3, pp. 96–105, (2017).
45. "jamovi - open statistical software for the desktop and cloud." Accessed: Mar. 01, 2024. [Online]. Available: https://www.jamovi.org/
46. "The Comprehensive R Archive Network." Accessed: Mar. 18, 2024. [Online]. Available: https://cran.r-project.org/